Direct Simulation Monte Carlo for Atmospheric Entry

2. Code Development and Application Results

Iain D. Boyd
Department of Aerospace Engineering
University of Michigan
Ann Arbor, Michigan, USA

iainboyd@umich.edu

ABSTRACT

The direct simulation Monte Carlo method (DSMC) has evolved over 40 years into a powerful numerical technique for the computation of complex, nonequilibrium gas flows. In this context, nonequilibrium means that the velocity distribution function is not in an equilibrium form due to a low number of intermolecular collisions within a fluid element. In atmospheric entry, nonequilibrium conditions occur at high altitude and in regions of flow fields with small length scales. In this second article of two parts, several different implementations of the DSMC technique in various, widely used codes are described. Validation of the DSMC technique for hypersonic flows using data measured in the laboratory is discussed. A review is then provided of the application of the DSMC technique to atmospheric entry flows. Illustrations of DSMC analyses are provided for slender and blunt body vehicles for entry into Earth, followed by examples of DSMC modeling of planetary entry flows.

1.0 INTRODUCTION

The direct simulation Monte Carlo (DSMC) method was first introduced by Graeme Bird in 1961 [1]. Since that time, Bird has written two books on the method [2,3] and thousands of research papers have been published that report on development and application of the technique. The DSMC method is most useful for analysis of kinetic nonequilibrium gas flows. In this context, nonequilibrium indicates that the velocity distribution function (VDF) of the gas molecules is not in the well-understood, Maxwellian, equilibrium form. The physical mechanism that pushes the VDF towards equilibrium is inter-molecular collisions, and so a gas falls into a nonequilibrium state under conditions where there is not a large enough number of collisions occurring to maintain equilibrium. The two main physical flow conditions that lead to nonequilibrium are low density and small length scales. A low density leads to a reduced collision rate while a small length scale reduces the size of a fluid element. The usual metric for determining whether a particular gas flow is in a state of nonequilibrium is the Knudsen number defined as follows:

$$Kn = \frac{\lambda}{L} \tag{1.1}$$

where λ is the mean free path of the gas and L is the characteristic length scale. The mean free path is the average distance traveled by each particle between collisions and is given for a hard sphere by

Report Documentation Page

Form Approved
OMB No. 0704-0188

1. REPORT DATE	2. REPORT TYPE	3. DATES COVERED
SEP 2009	**N/A**	**-**

4. TITLE AND SUBTITLE	5a. CONTRACT NUMBER
Direct Simulation Monte Carlo for Atmospheric Entry 2. Code Development and Application Results	5b. GRANT NUMBER
	5c. PROGRAM ELEMENT NUMBER
6. AUTHOR(S)	5d. PROJECT NUMBER
	5e. TASK NUMBER
	5f. WORK UNIT NUMBER
7. PERFORMING ORGANIZATION NAME(S) AND ADDRESS(ES) **Department of Aerospace Engineering University of Michigan Ann Arbor, Michigan, USA**	8. PERFORMING ORGANIZATION REPORT NUMBER
9. SPONSORING/MONITORING AGENCY NAME(S) AND ADDRESS(ES)	10. SPONSOR/MONITOR'S ACRONYM(S)
	11. SPONSOR/MONITOR'S REPORT NUMBER(S)

12. DISTRIBUTION/AVAILABILITY STATEMENT
Approved for public release, distribution unlimited

13. SUPPLEMENTARY NOTES
See also ADA562449. RTO-EN-AVT-162, Non-Equilibrium Gas Dynamics - From Physical Models to Hypersonic Flights (Dynamique des gaz non- equilibres - Des modeles physiques jusqu'au vol hypersonique)., The original document contains color images.

14. ABSTRACT
The direct simulation Monte Carlo method (DSMC) has evolved over 40 years into a powerful numerical technique for the computation of complex, nonequilibrium gas flows. In this context, nonequilibrium means that the velocity distribution function is not in an equilibrium form due to a low number of intermolecular collisions within a fluid element. In atmospheric entry, nonequilibrium conditions occur at high altitude and in regions of flow fields with small length scales. In this second article of two parts, several different implementations of the DSMC technique in various, widely used codes are described. Validation of the DSMC technique for hypersonic flows using data measured in the laboratory is discussed. A review is then provided of the application of the DSMC technique to atmospheric entry flows. Illustrations of DSMC analyses are provided for slender and blunt body vehicles for entry into Earth, followed by examples of DSMC modeling of planetary entry flows.

15. SUBJECT TERMS

16. SECURITY CLASSIFICATION OF:			17. LIMITATION OF ABSTRACT	18. NUMBER OF PAGES	19a. NAME OF RESPONSIBLE PERSON
a. REPORT	b. ABSTRACT	c. THIS PAGE			
unclassified	**unclassified**	**unclassified**	**SAR**	**28**	

$$\lambda = \frac{1}{\sqrt{2} n \sigma} \tag{1.2}$$

where n is the number density, and σ is the hard sphere collision cross section. Thus, at low density, the mean free path (and therefore Kn) becomes large. Similarly, for small length scales, L becomes small and again Kn becomes large. As a guiding rule, it is generally accepted that kinetic nonequilibrium effects become important when $Kn > 0.01$.

Atmospheric entry flow conditions may fall into the kinetic nonequilibrium regime at sufficiently low density (that occurs at high altitude in a planet's atmosphere) and for very small entry shapes (e.g. meteoroids that have a diameter on the order of a centimeter [4]). In addition, situations arise where localized regions of a flow may contain low density (e.g. the wake behind a capsule) or small length scales (e.g. sharp leading edges on a vehicle, or shock waves and boundary layers that may have very steep spatial gradients in flow field properties). Analysis of high Knudsen number flows could in principle be performed through solution of the Boltzmann equation, that is the fundamental mathematical model of dilute gas dynamics [3]. However, development of robust and general numerical solution schemes for the Boltzmann equation has proved a significant challenge. The DSMC technique emulates the same physics as the Boltzmann equation without providing a direct solution. The DSMC method follows a representative set of particles as they collide and move in physical space. It has been demonstrated that DSMC converges to solution of the Boltzmann equation in the limit of a very large number of particles [3].

In part one of this article [5], the fundamental aspects of the DSMC technique are first described with an emphasis on physical modeling issues related to its application to hypersonic, atmospheric entry problems. In this second article, the capabilities of the DSMC method are illustrated with regards to simulation of hypersonic, laboratory experiments and then to several different vehicle entry applications: (1) Earth entry of slender vehicles; (2) Earth entry of blunt vehicles; and (3) entry into planetary atmospheres. These studies will illustrate that the DSMC technique has been verified using several different sets of entry flight data. The level of confidence in the accuracy of the DSMC technique has reached the stage where it is now routinely employed for pre-mission design and post-mission data analysis of atmospheric entry flows.

2.0 FUNDAMENTAL ASPECTS OF THE DSMC TECHNIQUE

2.1 General Features

The DSMC technique emulates the physics of the Boltzmann equation by following the motions and collisions of a large number of model particles. Each particle possesses molecular level information including a position vector, a velocity vector, and physical information such as mass and size. Particle motion and collisions are decoupled over a time step Δt that is smaller than the local mean free time. During the movement of particles, boundary conditions such as reflection from solid surfaces are applied. The physical domain to be simulated in a DSMC computation is covered by a mesh of cells. These cells are used to collect together particles that may collide. There are a number of DSMC schemes for simulating collisions and all of them achieve a faster numerical performance than the molecular dynamics (MD) method [6] by ignoring the influence of the relative positions of particles within a cell in determining particles that collide. This simplification requires that the size of each cell be less than the local mean free path of the flow. Bird's No Time Counter (NTC) scheme [3] is the most widely used collision scheme in which a number of particle pairs in a cell are formed. Each of the pairs of particles is formed at random regardless of position within the cell, and then a probability of collision for each pair is evaluated using the product of the collision cross section and the relative velocity of the particle pair. This procedure reproduces the expected equilibrium collision rate under conditions of

equilibrium. A number of collision cross section models have been develop for DSMC, with the most widely used forms being the Variable Hard Sphere (VHS) [7] and the Variable Soft Sphere (VSS) [8]. For hypersonic flow, VHS is considered sufficiently accurate. Values of the VHS and VSS collision parameters for many common species are provided in Bird [3]. It is determined whether the particle pair actually collides by comparing the collision probability to a random number. When a collision occurs, post-collision velocities are calculated using conservation of momentum and energy. For the VHS model, isotropic scattering is assumed in which the unit vector of the relative velocity is assigned at random on the unit sphere.

The cells employed for simulating collisions are also often used for the sampling of macroscopic flow properties such as density, velocity, and temperature. There is no necessity to have the collision and sampling cells be identical, however, and sometimes a coarser mesh is used for sampling.

The basic steps in each iteration of the DSMC method are: (1) move particles over the time step Δt; (2) apply boundary conditions such as introducing new particles at inflow boundaries, removing particles at outflow boundaries, and processing reflections at solid boundaries; (3) sort particles into cells and calculate collisions; and (4) sample average particle information. A simulation will begin from some initial condition, and it will require a finite number of iterations for the flow to reach a steady state. Generally, steady state is detected as a leveling off of the total number of particles in the simulation. After steady state is reached, the simulation is continued a further number of iterations in order to reduce the statistical noise in the sampled information to an acceptable level. A typical DSMC computation may employ one million particles, reach steady state after 50,000 iterations, and continue sampling for a further 50,000 iterations. On a modern desktop computer, such a simulation should take about 3 hours.

While the ideas behind the DSMC technique are simple, implementation in an algorithm takes on many different forms. Specific DSMC algorithms have been developed for vector computers [9] and parallel computers [10,11]. Bird has focused work on customizing the algorithm to achieve efficient performance on single processor machines [12].

Having provided a general overview of the basic elements of the DSMC method, the reader is referred to the first article [5] where a more detailed review is provided of the physical models used in DSMC that are most critical to the analysis of hypersonic entry flows.

2.2 DSMC Codes

Unlike CFD, there are a relatively small number of different implementations of the above fundamental DSMC ideas in numerical codes. Among the most widely used DSMC codes for hypersonic entry analysis are DS2V/3V [13], DAC [11], SMILE [14], and MONACO [10]. These codes vary mainly in the treatment of collision selection methods and mesh topology (from orthogonal cut-cells to body-fitted unstructured cells). Most of the codes are parallelized and three-dimensional. Results from all of these codes for analysis of hypersonic entry flows are included in the following section.

DS2V/3V continues to undergo development by Bird [13]. The code uses a substructure of orthogonal cells to rapidly locate particles in the flow domain. A cut-cell treatment is used for definition of general surface elements. The No Time Counter technique is used for collisions. The code is not parallelized but runs very efficiently on desktop computers. New DSMC algorithms aimed at improving efficiency and quality of solution have recently been implemented [13]. The codes have been used extensively at NASA Langley Research Center to analyze both Earth and Mars entries.

DAC was developed at NASA Johnson Space Flight Center by LeBeau [11]. In 3D, DAC uses a surface mesh of triangular elements embedded within a Cartesian mesh for the flow field. The code is effectively parallelized with dynamic domain decomposition. DAC has been used extensively at NASA Langley Research Center particularly for 3D flow analyses of Earth and Mars entry flows.

SMILE has been developed in Russia over many years by Ivanov and his colleagues [14]. The code has a general user interface, is parallelized, and once again uses a background mesh of orthogonal cells with special treatment of surfaces. For simulating collision rates, it uses the majorant frequency scheme [14]. SMILE has been used to analyze the Earth entry of several capsules as well as the Mir space station.

MONACO has been under development since 1996 by Boyd and his colleagues [10]. The code uses body-fitted, unstructured meshes, and the No Time Counter method. This approach is less efficient than the orthogonal cut-cell method, but gives the code more generality. For example, the use of a generalized cell approach has greatly facilitated the merging of MONACO with the Particle-In-Cell (PIC) technique [15] for simulating collisional plasmas [16], and with Computational Fluid Dynamics (CFD) solving the Navier-Stokes equations for simulating hypersonic flows consisting of mixed regions of rarefied and continuum flow [17]. MONACO is very efficiently parallelized and has been applied to the analysis of a number of Earth entry flows.

3.0 DSMC ANALYSIS OF HYPERSONIC ENTRY FLOWS

In the following sections, a review is provided of the status of the application of the DSMC technique to hypersonic, entry flows. We first consider the application of DSMC to analyze hypersonic experiments conducted in ground-based facilities. Next, use of DSMC to analyze Earth entry flows is divided into slender and blunt body vehicle configurations. Finally, a summary of the use of DSMC for analysis of planetary entry is provided.

3.1 DSMC Analyses of Hypersonic Laboratory Experiments

Generation of rarefied, hypersonic flows in ground-based facilities presents a technical challenge, and very few data sets exist that enable a detailed assessment of DSMC codes. One notable code validation activity resulted from a NATO-AGARD working group on hypersonics. A planetary probe geometry was tested under rarefied, hypersonic flow conditions in several different experimental facilities and a number of research groups generated DSMC results for comparison. Many articles have been published on these studies and details of the experiments and numerical results are summarized in [18]. Examples of results obtained using the MONACO DSMC code are provided in Figs. 1a through 1c. Figure 1a shows the unstructured mesh that has been adapted to the local mean free path for the experiment conducted in the SR3 wind-tunnel in nitrogen at a Mach number of 20 and a Knudsen number of 0.03 [19]. Despite the high Mach number, this was a low-enthalpy facility with a total temperature of 1,100 K. Thus, neither vibrational relaxation nor chemistry occurs in these flows. While such experiments provide the opportunity to assess the collision cross sections (VHS, VSS) and rotational relaxation models [20], they provide no insight on the DSMC models for vibrational relaxation [21], and chemistry [22]. An electron beam diagnostic was employed in the SR3 wind-tunnel to measure the density field around the capsule geometry and Fig. 1b shows the excellent agreement obtained between DSMC and the measured data. Another experiment was conducted using the same geometry in the LENS facility again in nitrogen at a Mach number of 15.6 and a Knudsen number of 0.002 [23]. This higher enthalpy experiment had a total temperature of 4,350 K so that vibration was activated but there was still no chemistry. Figure 1c shows comparisons between measurements from LENS and DSMC computation

for the heat flux along the surface of the probe. Again, excellent agreement is obtained. While studies of this type indicate that the DSMC method is an accurate simulation method, the flows are not energetic enough to permit detailed assessment of DSMC thermochemical models.

Another code validation exercise (for both DSMC and CFD) was organized by Dr. Michael Holden of CUBRC and focused on hypersonic viscous interactions that can be generated on slender body configurations. A series of experiments was performed in the LENS facility for a number of configurations including double cones, and cylinder-flares [24]. While several groups performed DSMC analyses of some of these cases, Moss and Bird [22] provide the most comprehensive comparisons with the measured data. Figures 2a and 2b show comparisons for surface pressure and heat flux for a Mach 15.6, Kn=0.001 flow of nitrogen over a double cone configuration. DSMC results from two different codes (DS2V and SMILE) are provided and clearly give excellent agreement with the measurements. Similar levels of agreement between DS2V DSMC computations and measurements of pressure and heat flux are also shown in [25] for a Mach 12.4, Kn=0.0004 flow of nitrogen over a cylinder flare configuration. Similar to the planetary probe case, while vibrational energy of nitrogen was barely activated, there was no chemistry present in these flows.

There are very few comprehensive data sets measured under rarefied conditions involving three dimensional flows. An interesting example concerns data obtained in a low density, hypersonic wind-tunnel in the 1960's as part of the Apollo program [26-29]. A variety of very small models were tested that represented cones as well as capsules such as Apollo, Gemini, and Mercury. The MONACO DSMC code was applied to simulate the tests on the cones that were conducted in a Mach 10 flow of nitrogen at a global Knudsen number of 0.065 [30]. Figure 3a shows contours of Mach number computed for an angle of attack of 20 deg.. Figures 3b and 3c show comparisons for aerodynamic properties between measurement and simulation. In these figures, "FMF" shows results obtained from free molecular theory, and "MN" indicates modified Newtonian theory. For both the drag and the pitching moment, the 3D DSMC computations are in excellent agreement with the measured data. The comparisons also indicate that neither the free molecular theory nor the Newtonian theory provide any useful results for this condition indicating that the more computationally expensive DSMC approach is required. Figures 4a, 4b, and 4c show the corresponding results for Mach 10 flow of nitrogen over a model of the Apollo Command Module capsule at a Knudsen number of 0.067 conducted in the exact same facility as the cone studies. In this case, significant differences between simulation and measurement are found for the drag force. Similarly, there is relatively poor agreement between the MONACO DSMC solutions for pitching moment coefficient and the measured values, as shown in Fig. 4c. For example, DSMC predicts a trim angle that is about 15 deg. different from the experiments. Independent DSMC computations of the same flows were performed using the DS3V DSMC code, and the results show excellent agreement with the MONACO DSMC profiles. The fact that good agreement between measurement and simulation is obtained in one case and not in another for two tests performed in the same experimental facility illustrates the difficulties involved in validating the DSMC approach using the limited amounts of laboratory data. This situation clearly calls out for additional experiments to be carried out carefully under hypersonic, rarefied flow conditions.

Despite the lack of detailed validation using laboratory data, the DSMC technique has been applied to analyze the aerodynamics and aerothermodynamics of many different spacecraft entering the atmospheres of Earth and of planets in the Solar System. In the following sections, we provide a review of prior DSMC studies of atmospheric entry that is divided into three parts: (1) Earth entry of slender bodies; (2) Earth entry of blunt bodies; and (3) planetary entry.

3.2 DSMC Analyses of Earth Entry Flows

The review of previous DSMC analyses of Earth entry flows is divided into those related to defense applications and those related to return of payloads from space. These two classes of entry missions involve very different trajectories and vehicle configurations.

3.2.1 Slender Body Configurations

Very high speed delivery of military payloads is achieved using slender vehicle geometries. The Bow-Shock Ultra-Violet-2 (BSUV-2) hypersonic flight experiment represents an example of such a vehicle that was flown in 1991 [31]. The vehicle geometry consisted of a spherically-capped 15 deg. cone with a nose radius of about 10 cm. BSUV-2 reentered the atmosphere at 5.1 km/sec and provided data in the altitude range from 110 to 60 km. Experimental measurements of the ultra-violet emission due to nitric oxide and vacuum-ultra-violet emission due to atomic oxygen resonance transitions were obtained by on-board instrumentation. Calculation of the radiative emission was performed in a decoupled approach. The chemically reacting flow field was computed using both continuum (CFD) [32,33,34] and direct simulation Monte Carlo (DSMC) methods [34]. Then, the emission was predicted from the flow field solutions using the NASA nonequilibrium radiation code NEQAIR [35]. Initial comparisons between DSMC-based results and measurement are labelled (1993) in Fig. 5a and produced poor agreement at high altitude. This led to significant activity in the study of the oxygen dissociation and nitric oxide formation chemistry models used in the DSMC computations [36,37]. The final results obtained for nitric oxide radiance as a function of altitude are labelled “new models” in Fig. 5a [38]. Note that the BSUV-2 Knudsen number ranged from 0.008 at 71 km to 0.215 at 90 km. In addition to obtaining very good agreement with radiance, the spectral features were also reproduced extremely well in the computations as demonstrated in Fig. 5b. Good agreement was also obtained between DSMC-based prediction and measurement for atomic oxygen emission as shown in Fig. 5c. Sensitivity to the gas-surface interaction model used in DSMC is assessed through variation of the accommodation coefficient, α_t. The BSUV-2 studies clearly illustrated that access to detailed experimental measurements are needed in order to make significant advances in thermochemical modeling using the DSMC technique.

The Radio Attenuation Measurement (RAM) experiments involved a series of hypersonic entry flights designed to study communications blackout. This is an important operational issue for all hypersonic vehicles in which the plasma formed at very high speed interferes with radio waves sent to and from the vehicle. The vehicle of interest here (RAM-C II), consisted of a cone with a spherical nose cap of radius 0.1524 m, a cone angle of 9 deg., and a total length of about 1.3 m. While entering at orbital velocity (7.8 km/s), the RAM-C II experiment made measurements from about 90 km to 60 km altitude. Electron number density was measured using two different diagnostics at several locations in the plasma layer surrounding the vehicle [39,40]. A series of reflectometers was used to measure the maximum plasma density along lines normal to the vehicle surface in four different locations. A rake of Langmuir probes measured variation in the plasma density across the plasma layer near the rear of the vehicle. A schematic diagram of the vehicle geometry and the instrumentation placement is shown in Fig. 6a. DSMC analysis of the RAM-C experiment at 81 km was performed by Boyd [41] in order to make assessment of DSMC procedures for simulating charged species (electrons, ions) in trace amounts. The DSMC results were compared directly with the measurements of plasma density taken on the RAM-C II flight and these are shown in Figs. 6b and 6c. In each case, the sensitivity of the DSMC results to the model (TCE or VFD) employed for dissociation chemistry is investigated. Clearly, very good agreement is obtained between simulation and measurement that provided validation of the new DSMC procedures.

3.2.2 Blunt Body Configurations

The successful return of payloads (including people) from space requires use of blunt vehicle geometries to provide reduced levels of deceleration and heat load. One of the first applications of the DSMC technique to analyze the entry aerodynamics of a full-scale vehicle was performed by Rault [42] who simulated the aerodynamics of the Space Shuttle Orbiter at altitudes from 170 to 100 km where the Knudsen number ranged from about 2 to 0.005. Performed around 1993, these 3D computations were extremely expensive for the time. Comparison of the results obtained was made with free molecular theory, with CFD calculations, with aerodynamic bridging relations, and with Space Shuttle flight data. Very good agreement was obtained between DSMC and flight data for lift-to-drag ratio and for the axial force coefficient. Significant discrepancies were, however, found both for the normal force coefficient and for the pitching moment.

Ivanov et al. [43] describe DSMC analysis using SMILE of the aerodynamics of a Russian entry capsule over the altitude range from 130 to 85 km. Comparisons made between the DSMC results and free flight experimental measurements for the axial and normal force and pitching moment coefficients revealed excellent agreement. The SMILE code was also applied by Markelov et al. [44] to help in the analysis of de-orbiting the Russian space station Mir. The highly complex, 3D geometry was analyzed using DSMC over the altitude range from 200 to 110 km for which the effective Knudsen number varies from about 20 to 0.05. It was found that aerodynamic coefficients do not change significantly until about 120 km and that the vehicle is statically stable throughout this altitude range.

Moss [45] applied the DS2V DSMC code to analyze the aerothermodynamics of a proposed ballute deceleration system for Earth entry at velocities from 14 to 7 km/s and altitudes from 200 to 100 km. A schematic diagram of the capsule-ballute configuration is shown in Fig. 7a. An example of the complex flow computed using DSMC is provided in Fig. 7b. A number of interesting and important conclusions were drawn from the analyses including the observation of unsteady flow phenomena for certain capsule-ballute configurations, and that the highest heat fluxes were experienced on the ballute tether.

A DSMC study using both DS3V and DAC of a lower speed entry was performed by Moss et al. [46] to analyze the supersonic aerodynamics in the transition regime of NASA's Inflatable Reentry Vehicle Experiment (IRVE). The DSMC technique was employed to develop an extensive aerodynamics database covering the altitude range from 150 to 95 km for which the vehicle Knudsen number ranged from 10 to 0.017. Angle of attack was varied from 0 to 180 deg.. Another high altitude supersonic flight experiment called TOMEX was analyzed using the MONACO DSMC code by Sun et al. [47]. Three dimensional computations of the complex vehicle geometry were performed that included the flow into pressure sensors employed during flight. The Knudsen number ranged from about 50 to 0.02. As a demonstration of the strong capabilities of the DSMC technique to model complex, 3D flow configurations, a side view of the flow field mesh that employs tetrahedral cells is shown in Fig. 8a for one of the TOMEX cases. Figure 8b illustrates the excellent agreement that was obtained between the DSMC predictions and the pressures measured by several different sensors during the TOMEX flight.

NASA's Stardust Sample Return Capsule (SRC) entered the Earth's atmosphere at a velocity of about 12.8 km/s making it the most energetic man-made vehicle to undergo hypersonic entry. The SRC geometry is shown in Fig. 9a. The DSMC codes G2 (an earlier form of Bird's DS2V code) and DAC were used by Wilmoth et al. [48] prior to the flight in 1998 in order to analyze the entry aerodynamics. Focused on aerodynamics, those early Stardust DSMC computations omitted ionization and employed simple thermochemical models. During the SRC entry in 2006, a suite of spectroscopic instruments measured the radiation emitted from the very strong bow shock wave formed around the vehicle [49]. With the availability

of detailed experimental measurements, several further DSMC studies of the SRC entry have been performed recently that employed state-of-the-art thermochemistry modeling including ionization [50,51,52]. Profiles of the temperatures from the various energy modes (Tt=translation; Tr=rotational; Tv=vibrational; Te=electron) predicted along the stagnation streamline of the SRC at an altitude of 81 km are shown in Fig. 9b. The separation among these profiles illustrates the strong degree of thermal nonequilibrium of the gas under these extreme conditions. Profiles along the stagnation streamline of the mole fractions of selected chemical species are shown in Fig. 9c illustrating the high degree of chemical activity present in the flow. The NEQAIR radiation code [35] was again employed to estimate the radiation spectra based on the DSMC flow field results. An example of a direct comparison between the computed and measured spectra at an altitude of 81 km is shown in Fig. 9d. Generally, it is found that air plasma atomic line features are quite well predicted by the combination of DSMC and NEQAIR.

3.3 DSMC Analyses of Planetary Entry Flows

Several DSMC studies have been performed of the aerodynamics and heating of vehicles entering the Mars atmosphere that consists of 95.4% of CO_2 and 4.6% of N_2. Direct comparisons between DSMC predictions obtained using DAC and flight measurements taken during the Viking-1 entry for the ratio of normal to axial aerodynamic force yielded excellent agreement as shown in Fig. 10 [53]. Similar comparisons for the drag coefficient indicated that the DSMC results were not inconsistent with the measurements although the flight data were only taken in the continuum regime so direct comparison with DSMC was not possible. An extensive aerodynamics database was constructed using G2 and DAC for the Mars Pathfinder mission by Moss et al. [54]. The DSMC analyses traversed a Knudsen number range from 100 to 0.027 and angle of attack variation from 0 to 35 deg.. The database was used for Martian atmosphere density reconstruction and spacecraft attitude determination based on in-flight accelerometer data. DAC was again used by Wilmoth et al. [55] to analyze the aerothermodynamics of the Mars Global Surveyor (MGS). The data generated were employed for spacecraft design, mission planning, flight operations, and atmospheric reconstruction. MGS was the first planetary entry mission designed to use aerobraking to customize its orbit by gradually descending into the Mars atmosphere over a period of several months. The Knudsen number during the aerobraking process varied from about 10 down to 0.05 placing the flows firmly in the transition regime. The DSMC generated aerothermodynamic database played a key role in the successful completion of the aerobraking maneuver. Finally, the DAC and G2 DSMC codes were applied by Moss et al. [56] to generate an aerothermodynamic database for Mars Microprobes. Aerodynamics characteristics and surface heat flux were determined over a Knudsen number range from 80 to 0.002.

DSMC analyses have been performed on the interaction of the Magellan spacecraft with the atmosphere of Venus. The composition of the Venusian atmosphere is 76% CO_2, 9% CO, 9% Ar, and 6% N_2. Near the end of its mission, the Magellan spacecraft for the first time successfully performed an aero-brake maneuver in the atmosphere to circularize its orbit. Rault [57] applied a 3D DSMC code to compute the aerodynamic characteristics of the complex spacecraft geometry at an altitude of 140 km as part of the assessment of whether to perform the aero-brake maneuver. The complex mesh is illustrated in Fig. 11a. The flow had a freestream Knudsen number of about 10 and the DSMC results indeed showed only minor departures from free molecular analysis. Contours of density ratio (ρ/ρ_∞) at an angle of attack of 30 deg. and a 50 deg. roll are shown in Fig. 11b. A similar analysis was reported by Haas and Schmitt [58] using a different 3D DSMC code. They found relatively small differences of 5-10% between DSMC and free molecular theory for forces, moments, and heating. In a related study, Haas and Feiereisen [59] used DSMC to analyze the heating to the Magellan spacecraft during proposed aero-pass maneuvers.

DSMC analysis of the rarefied portion of the entry of the Galileo probe into the atmosphere of Jupiter was performed by Haas and Milos [60]. The Jovian atmosphere consists of 89% H_2 and 11% He. Seven points along the entry trajectory were investigated with the freestream Knudsen number ranging from 400 to 0.07 and all at zero angle of attack. The purpose of the analysis was to accurately compute the drag coefficient that was needed to infer atmospheric density from an accelerometer experiment. A unique aspect of this study was the coupling of the convective heating predictions from DSMC to a thermal response code in order to estimate out-gassing rates of pyrolyzed gas originating in the thermal protection system of the probe. The predicted flux of pyrolysis products was as much as an order of magnitude higher than the freestream flux and had a significant effect on the probe aerodynamics, for example reducing the drag coefficient by 15%.

4.0 SUMMARY

The direct simulation Monte Carlo method (DSMC) has evolved more than 40 years into a powerful analysis tool for computation of kinetic nonequilibrium hypersonic entry flows. The heart of the technique is its detailed treatment of collisional phenomena including relaxation of internal energy modes, chemistry, radiation, and gas-surface interaction. Assessment of the DSMC technique for hypersonic flows using ground-based experimental measurements has been limited to conditions without chemistry due to the technical challenges of generating high-energy, rarefied flows. The DSMC method has been validated using flight data (BSUV-2, RAM-C) for slender body vehicles based on measurements of radiation emission and plasma density. The DSMC technique has also been applied to analyze the entry into Earth's atmosphere of several different blunt body configurations including comparisons with flight measurements for the Space Shuttle, space station Mir, TOMEX, and Stardust. The DSMC technique generally provides excellent comparisons with most of the measured data sets. The confidence obtained in the physical accuracy of the DSMC method has led to its application to analyze the aerothermodynamic performance of proposed vehicles such as ballutes and to aid in the design of entry flight experiments such as IRVE. The DSMC technique has played a key role in the design and flight analysis of several NASA Mars entry missions including the entry of Pathfinder and the aerobraking of Mars Global Surveyor. Further notable applications of the DSMC technique to planetary entries include analysis of the aero-braking maneuver of the Magellan spacecraft in the atmosphere of Venus, and entry into Jupiter of the Galileo probe.

5.0 ACKNOWLEDGMENTS

The author gratefully acknowledges financial support from NASA through grants NCC3-989, NNX08AD02A, and NNX08AH37A.

6.0 REFERENCES

[1] Bird, G.A., "Approach to Translational Equilibrium in a Rigid Sphere Gas," *Physics of Fluids*, Vol. 6, 1963, pp. 1518-1519.

[2] Bird, G.A., *Molecular Gas Dynamics*, Oxford University Press, Oxford, 1976.

[3] Bird, G.A., *Molecular Gas Dynamics and the Direct Simulation of Gas Flows*, Oxford University Press, Oxford, 1994.

[4] Boyd, I.D., "Computation of Atmospheric Entry Flow About a Leonid Meteoroid," *Earth, Moon, and Planets*, Vol. 82, 2000, pp. 93-108.

[5] Boyd, I.D., "Direct Simulation Monte Carlo for Atmospheric Entry. 1: Theoretical Basis and Physical Models," notes for VKI Shortcourse, *Nonequilibrium Gas Dynamics: From Physical Models to Hypersonic Flights*, September 2008.

[6] Alder, B.J. and Wainwright, T.E., "Studies in Molecular Dynamics," *Journal of Chemical Physics*, Vol. 27, 1957, pp. 1208-1209.

[7] Bird, G.A., "Monte Carlo Simulation in an Engineering Context," *Progress in Astronautics and Aeronautics*, Vol. 74, AIAA, New York, 1981, pp. 239-255.

[8] Koura, K. and Matsumoto, H., "Variable Soft Sphere Molecular Model for Air Species," *Physics of Fluids A*, Vol. 4, 1992, pp. 1083-1085.

[9] Boyd, I.D., "Vectorization of a Monte Carlo Simulation Scheme for Nonequilibrium Gas Dynamics," *Journal of Computational Physics*, Vol. 96, 1991, pp. 411-427.

[10] Dietrich, S. and Boyd, I.D., "Scalar and Parallel Optimized Implementation of the Direct Simulation Monte Carlo Method," *Journal of Computational Physics*, Vol. 126, 1996, pp. 328-342.

[11] LeBeau, G. J., "A Parallel Implementation of the Direct Simulation Monte Carlo Method," *Computer Methods in Applied Mechanics and Engineering*, Vol. 174, 1999, pp. 319-337.

[12] Bird, G.A., "Sophisticated Versus Simple DSMC," Proceedings of the 25th International Symposium on Rarefied Gas Dynamics, St. Petersburg, Russia, July 2006.

[13] Bird, G.A., "The DS2V/3V Program Suite for DSMC Calculations," *Rarefied Gas Dynamics, 24th International Symposium*, Vol. 762, edited by M. Capitelli, American Institute of Physics, Melville, NY, 2005, pp. 541-546.

[14] Ivanov, M.S., Markelov, G.N., and Gimelshein, S.F., "Statistical Simulation of Reactive Rarefied Flows: Numerical Approach and Applications," AIAA Paper 98-2669, June 1998.

[15] Birdsall, C.K. and Langdon, A.B., *Plasma Physics Via Particle Simulation*, Adam Hilger, 1991.

[16] Choi, Y., Keidar, M., and Boyd, I.D., "Particle Simulation of Plume Flows From an Anode-Layer Hall Thruster," *Journal of Propulsion and Power*, 2008, pp. 554-561.

[17] Schwartzentruber, T.E., Scalabrin, L.C., and Boyd, I.D., "Hybrid Particle-Continuum Simulations of Non-Equilibrium Hypersonic Blunt Body Flow Fields," *Journal of Thermophysics and Heat Transfer*, Vol. 22, 2008, pp. 29-37.

[18] Moss, J.N. and Price, J.M., "Survey of Blunt Body Flows Including Wakes at Hypersonic Low-Density Conditions," *Journal of Thermophysics and Heat Transfer*, Vol. 11, 1997, pp. 321-329.

[19] Allegre, J. and Birsch, D., "Blunted Cone at Rarefied Hypersonic Conditions – Experimental Density Flowfields, Heating Rates, and Aerodynamic Forces," CNRS Report, RC 95-2, 1995.

[20] Boyd, I.D., "Analysis of Rotational Nonequilibrium in Standing Shock Waves of Nitrogen," *AIAA Journal*, Vol. 28, 1990, pp. 1997-1999.

[21] Vijayakumar, P., Sun, Q. and Boyd, I.D., "Detailed Models of Vibrational-Translational Energy Exchange for the Direct Simulation Monte Carlo Method," *Physics of Fluids*, Vol. 11, 1999, pp. 2117-2126.

[22] Haas, B.L. and Boyd, I.D., "Models for Direct Monte Carlo Simulation of Coupled Vibration-Dissociation," *Physics of Fluids A*, Vol. 5, 1993, pp. 478-489.

[23] Holden, M., Kolly, J., and Chadwick, K., "Callibration, Validation, and Evaluation Studies in the LENS Facility," AIAA Paper 95-0291, 1995.

[24] Holden, M.S. and Wadhams, T.P., "Code Validation Study of Laminar Shock/Boundary layer and Shock/Shock Interactions in Hypersonic Flow. Part A: Experimental Measurements," AIAA Paper 2001-1031, January 2001.

[25] Moss, J.N. and Bird, G.A., "Direct Simulation Monte Carlo Simulations of Hypersonic Flows With Shock Interactions," *AIAA Journal*, Vol. 43, 2005, pp. 2565-2573.

[26] Boylan, D. E., and Potter, J. L., "Aerodynamics of Typical Lifting Bodies under Conditions Simulating Very High Altitudes," *AIAA Journal*, Vol. 5, 1967, pp..226-232.

[27] Griffith, B. J., "Comparison of Aerodynamic Data from the Gemini Flights and AEDC-VKF Wind Tunnels," *Journal of Spacecraft*, Vol. 4, No. 7, 1967, pp. 919-924.

[28] Griffith, B. J., and Boylan, D. E., "Reynolds and Mach Number Simulation of Apollo and Gemini Re-entry and Comparison with Flight," *Specialists' Meeting on Hypersonic Boundary Layers and Flow Fields of the Fluid Dynamics Panel of AGARD*, North Atlantic Treaty Organization, Paris, 1968, pp. 8-1−8-21.

[29] Boylan, D. E., and Griffith, B. J., "Simulation of the Apollo Command Module Aerodynamics at Re-entry Altitudes," *Proceedings of the 3rd National Conference on Aerospace Meteorology*, American Meteorological Society, Boston, 1968, pp.370-378.

[30] Padilla, J.F. and Boyd, I.D., "Assessment of Rarefied Hypersonic Aerodynamics Modeling and Windtunnel Data," AIAA Paper 2006-3390, June 2006.

[31] Erdman, P.W., Zipf, E.C., Espy, P., Howlett, L.C., Levin, D.A., Collins, R.J., and Candler, G.V., "Measurements of Ultraviolet Radiation From a 5-km/sec Bow Shock," *Journal of Thermophysics and Heat Transfer*, Vol. 8, 1994, pp. 441-446.

[32] Levin, D.A., Candler, G.V., Collins, R.J., Erdman, P.W., Zipf, E., and Howlett, L.C., "Examination of Ultraviolet Radiation Theory for Bow Shock Rocket Experiments-I," *Journal of Thermophysics and Heat Transfer*, Vol. 8, 1994, pp. 447-453.

[33] Levin, D.A., Candler, G.V., Howlett, L.C., and Whiting E.E., "Comparison of Theory With Atomic Oxygen 130.4 nm Radiation Data From the Bow Shock Ultraviolet 2 Rocket Flight," *Journal of Thermophysics and Heat Transfer*, Vol. 9, 1995, pp. 629-635.

[34] Candler, G.V., Boyd, I.D., and Levin, D.A., "Continuum and DSMC Analysis of Bow Shock Flight Experiments," AAA Paper 93-0275, January 1993.

[35] Whiting, E.E., Park, C., Liu, Y., Arnold, J.O., and Paterson, J.A., "NEQAIR96, Nonequilibrium and Equilibrium Radiative Transport and Spectra Program: User's Manual," *NASA Reference Publication 1389*, December 1996.

[36] Boyd, I.D., Candler, G.V., and Levin, D.A., "Dissociation Modeling in Low Density Hypersonic Flows of Air," *Physics of Fluids*, Vol. 7, 1995, pp. 1757-1763.

[37] Boyd, I.D., Bose, D., and Candler, G.V., "Monte Carlo Modeling of Nitric Oxide Formation Based on Quasi-Classical Trajectory Calculations," *Physics of Fluids*, Vol. 9, 1997, pp. 1162-1170.

[38] Boyd, I.D., Phillips, W.D., and Levin, D.A., "Sensitivity Studies for Prediction of Ultra-Violet Radiation in Nonequilibrium Hypersonic Bow-Shock Waves," *Journal of Thermophysics and Heat Transfer*, Vol. 12, 1998, pp. 38-44.

[39] Grantham, W.L., "Flight Results of a 25000 Foot Per Second Reentry Experiment Using Microwave Reflectometers to Measure Plasma Electron Density and Standoff Distance," *NASA Technical Note D-6062*, 1970.

[40] Linwood-Jones, W. and Cross, A.E., "Electrostatic Probe Measurements of Plasma Parameters for Two Reentry Flight Experiments at 25000 Feet Per Second," *NASA Technical Note D-6617*, 1972.

[41] Boyd, I.D., "Modeling of Associative Ionization Reactions in Hypersonic Rarefied Flows," *Physics of Fluids*, Vol. 19, 2007, Article 096102.

[42] Rault, D.F.G, "Aerodynamics of the Shuttle Orbiter at High Altitudes," *Journal of Spacecraft and Rockets*, Vol. 31, 1994, pp. 944-952.

[43] Ivanov, M.S., Markelov, G.N., Gimelshein, S.F., Mishina, L.V., Krylov, A.N., and Grechko, N.V., "High-Altitude Capsule Aerodynamics With Real Gas Effects," *Journal of Spacecraft and Rockets*, Vol. 35, 1998, pp. 16-22.

[44] Markelov, G.N., Kashkovsky, A.V., and Ivanov, M.S., "Space Station Mir Aerodynamics Along the Descent Trajectory," *Journal of Spacecraft and Rockets*, Vol. 38, 2001, pp. 43-50.

[45] Moss, J.N., "Direct Simulation Monte Carlo Simulations of Ballute Aerothermodynamics Under Hypersonic Rarefied Conditions," *Journal of Spacecraft and Rockets*, Vol. 44, 2007, pp. 289-298.

[46] Moss, J.N., Glass, C.E., Hollis, B.R., and Van Norman, J.W., "Low-Density Aerodynamics for the Inflatable Reentry Vehicle Experiment," *Journal of Spacecraft and Rockets*, Vol. 36, 2006, pp. 1191-1201.

[47] Sun, Q., Cai, C., Boyd, I.D., Clemmons, J.H. and Hecht, J.H., "Computational Analysis of High-Altitude Ionization Gauge Flight Measurements," *Journal of Spacecraft and Rockets*, Vol. 43, 2006, pp. 186-193.

[48] Wilmoth, R.G., Mitcheltree, R.A., and Moss, J.N., "Low-Density Aerodynamics of the Stardust Sample Return Capsule," *Journal of Spacecraft and Rockets*, Vol. 36, 1999, pp. 436-441.

[49] Jenniskens, P., "Observations of the STARDUST Sample Return Capsule Entry with a Slit-Less Echelle Spectrograph," AIAA Paper 2008-1210, January 2008.

[50] Ozawa, T., Zhong, J., Levin, D. A., Boger, D., and Wright, M. J., "Modeling of the Stardust Reentry Flows With Ionization in DSMC," AIAA Paper 2007-0611, January 2007.

[51] Boyd, I. D., Trumble, K., and Wright, M.J., "Nonequilibrium Particle and Continuum Analyses of Stardust Entry for Near-Continuum Conditions," AIAA Paper 2007-4543, June 2007.

[52] Boyd, I.D., Zhong, J., Levin, D.A., and Jenniskens, P., "Flow and Radiation Analyses for Stardust Entry at High Altitude," AIAA Paper 2008-1218, January 2008.

[53] Blanchard, R.C., Wilmoth, R.G., and Moss, J.N., "Aerodynamic Flight Measurements and Rarefied-Flow Simulations of Mars Entry Vehicles," *Journal of Spacecraft and Rockets*, Vol. 34, 1997, pp. 687-690.

[54] Moss, J.N., Blanchard, R.C., Wilmoth, R.G., and Braun, R.D., "Mars Pathfinder Rarefied Aerodynamics: Computations and Measurements," *Journal of Spacecraft and Rockets*, Vol. 36, 1999, pp. 330-339.

[55] Wilmoth, R.G., Rault, D.F.G., Cheatwood, F.M., Engelund, W.C., and Shane, R.W., "Rarefied Aerothermodynamic Predictions for Mars Global Surveyor," *Journal of Spacecraft and Rockets*, Vol. 36, 1999, pp. 314-322.

[56] Moss, J.N., Wilmoth, R.G., and Price, J.M., "Direct Simulation Monte Carlo Calculations of Aerothermodynamics for Mars Microprobe Capsules," *Journal of Spacecraft and Rockets*, Vol. 36, 1999, pp. 399-404.

[57] Rault, D.F.G, "Aerodynamic Characteristics of the Magellan Spacecraft in the Venus Upper Atmosphere," *Journal of Spacecraft and Rockets*, Vol. 31, 1994, pp. 537-542.

[58] Haas, B.L. and Schmitt, D.A., "Simulated Rarefied Aerodynamics of the Magellan Spacecraft During Aerobraking," *Journal of Spacecraft and Rockets*, Vol. 31, 1994, pp. 980-985.

[59] Haas, B.L. and Feiereisen, W.J., "Particle Simulation of Rarefied Aeropass Maneuvers of the Magellan Spacecraft," *Journal of Spacecraft and Rockets*, Vol. 31, 1994, pp. 17-24.

[60] Haas, B.L. and Milos, F.S., "Simulated Rarefied Entry of the Galileo Probe into the Jovian Atmosphere," *Journal of Spacecraft and Rockets*, Vol. 32, 1995, pp. 398-403.

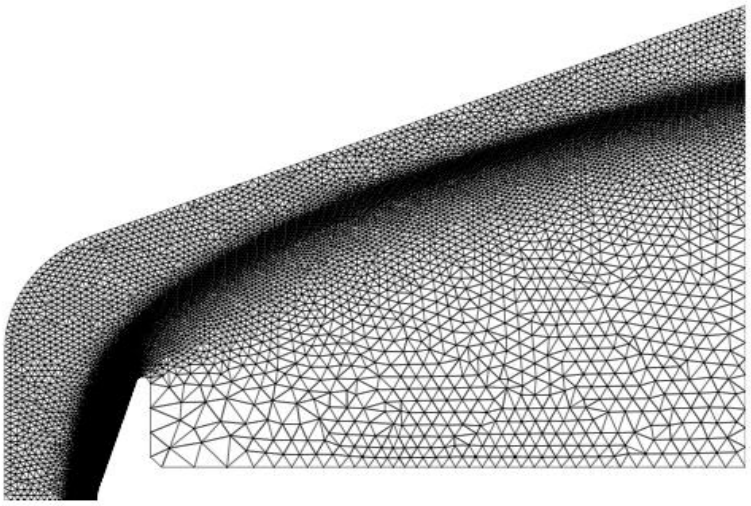

Figure 1a: Adapted mesh for Mach 20, Kn=0.03 flow over a planetary probe.

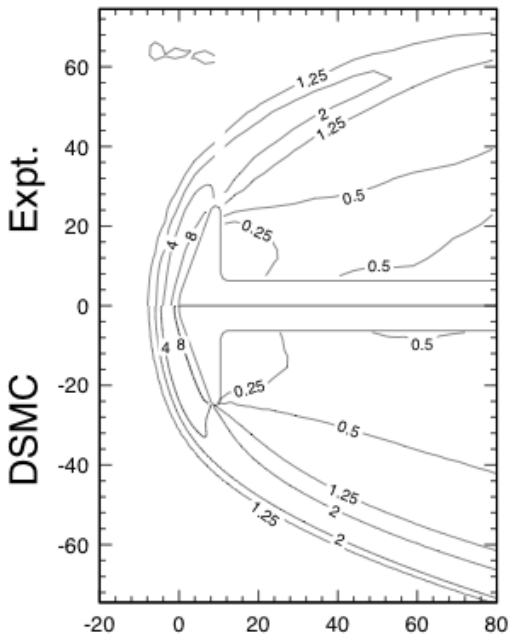

Figure 1b: Contours of ρ/ρ_∞ for Mach 20, Kn=0.03 flow over a planetary probe [19].

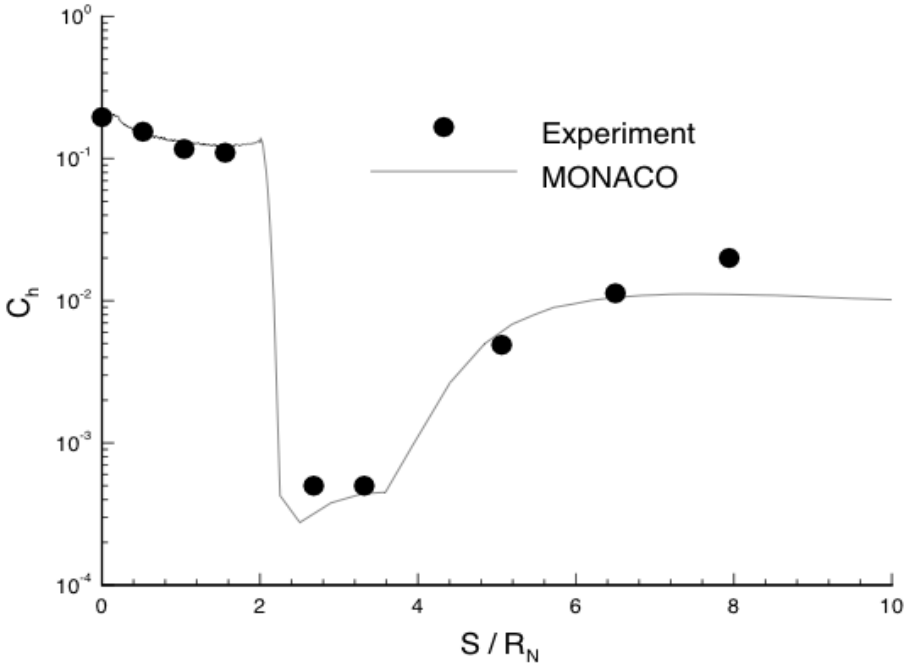

Figure 1c: Heat flux coefficient on a planetary probe at Mach 15.6, Kn=0.002 [19].

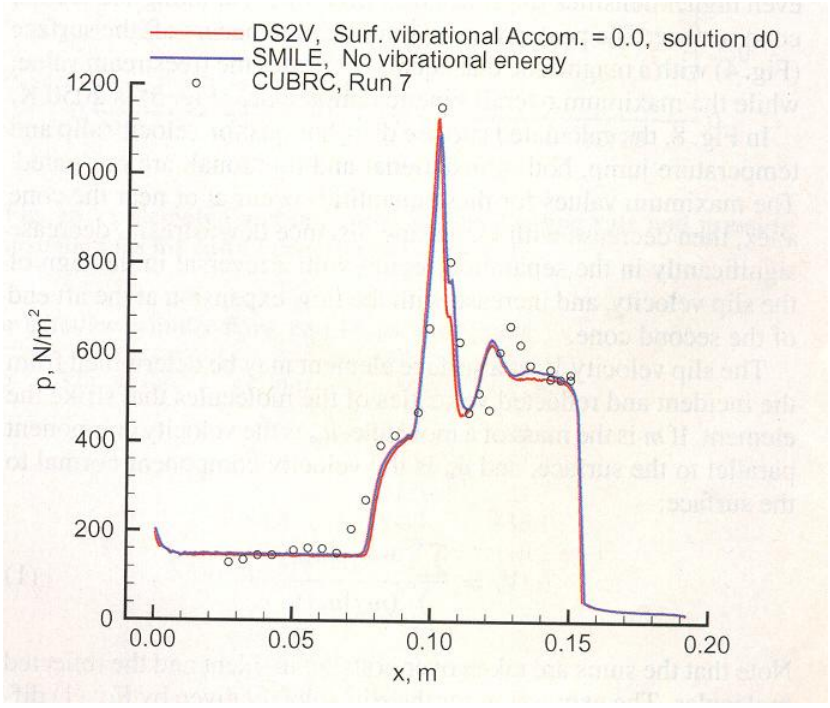

Figure 2a: Pressure along the surface of a double cone tested at Mach 15.6, Kn=0.002 [25].

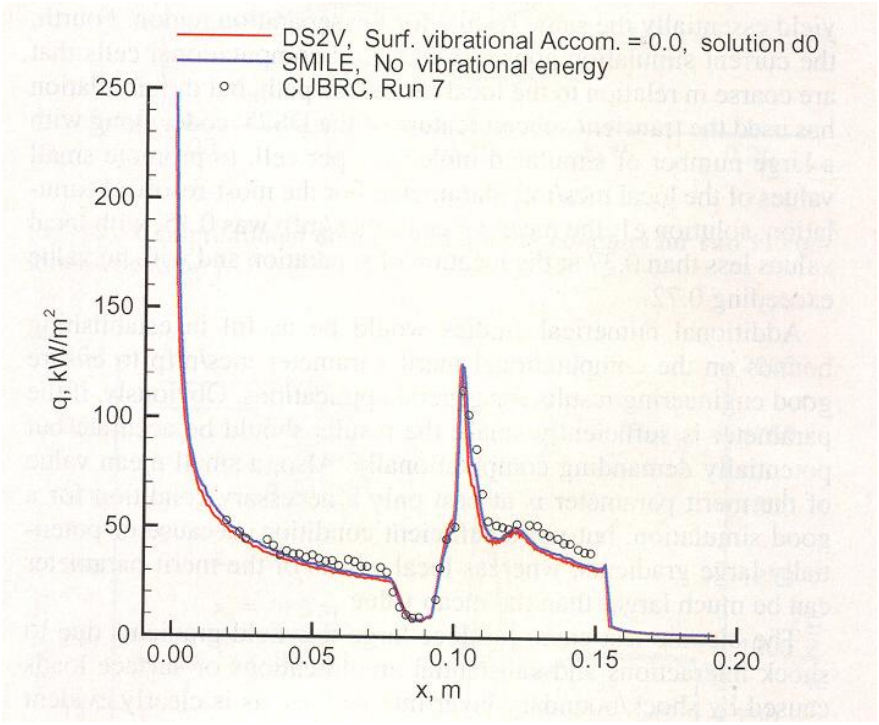

Figure 2b: Heat flux along the surface of a double cone tested at Mach 15.6, Kn=0.002 [25].

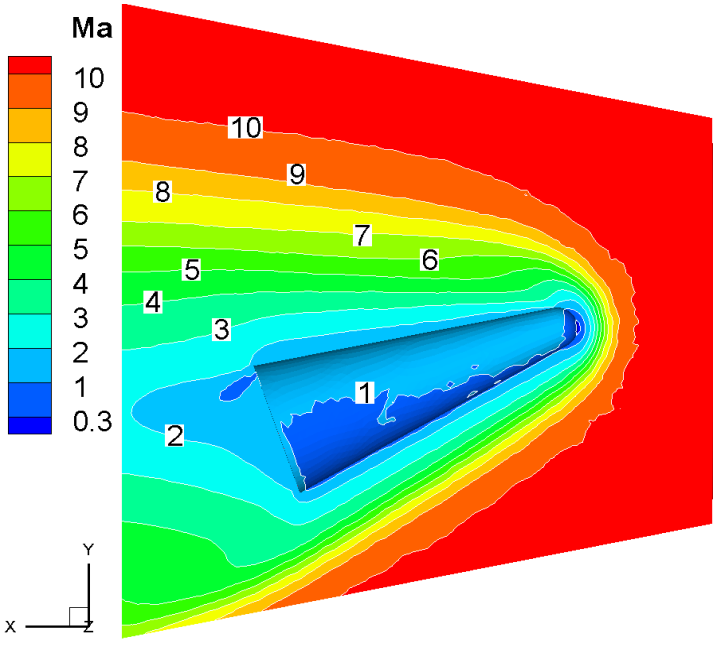

Figure 3a: Contours of Mach number about a cone at angle of attack [30].

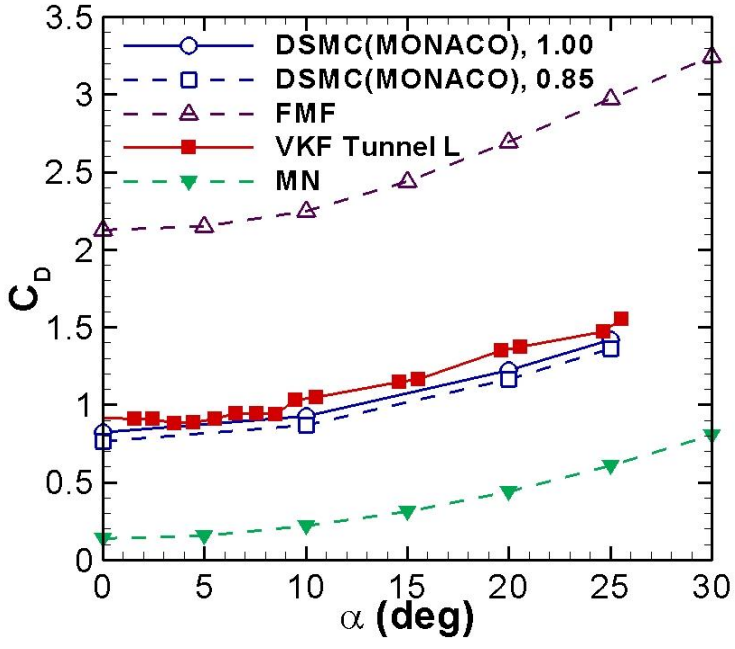

Figure 3b: Drag coefficient for a cone at angle of attack [30].

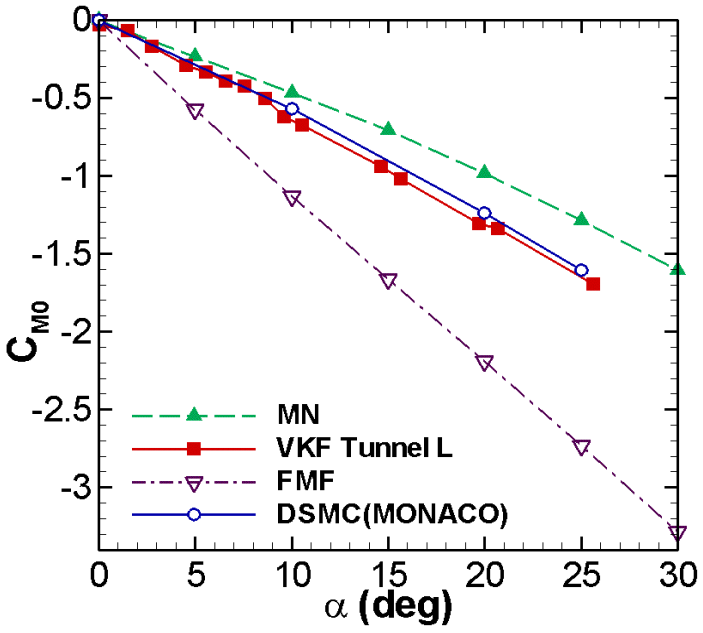

Figure 3c: Pitching moment for a cone at angle of attack [30].

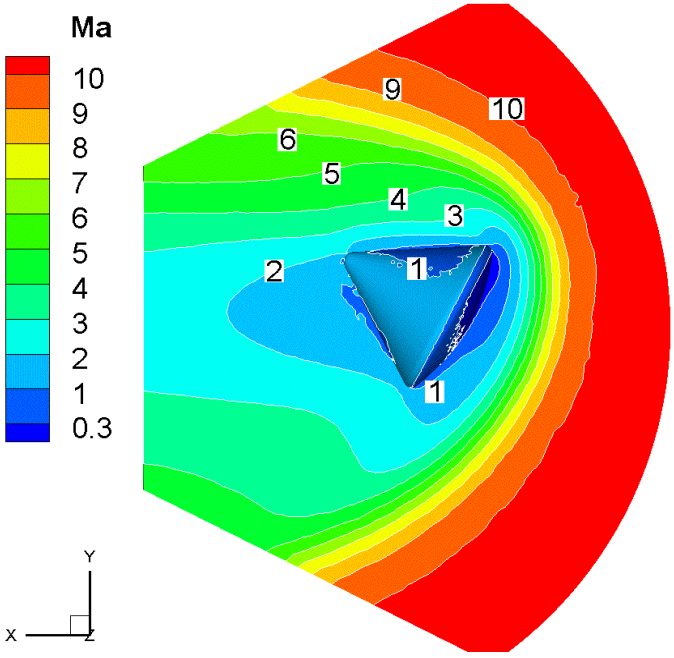

Figure 4a: Contours of Mach number about a capsule at angle of attack [30].

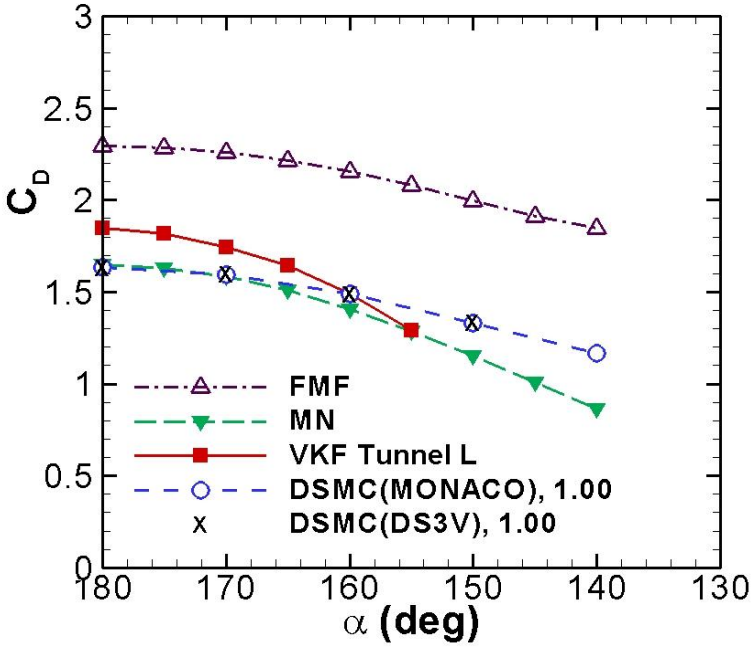

Figure 4b: Drag coefficient for a capsule at angle of attack [30].

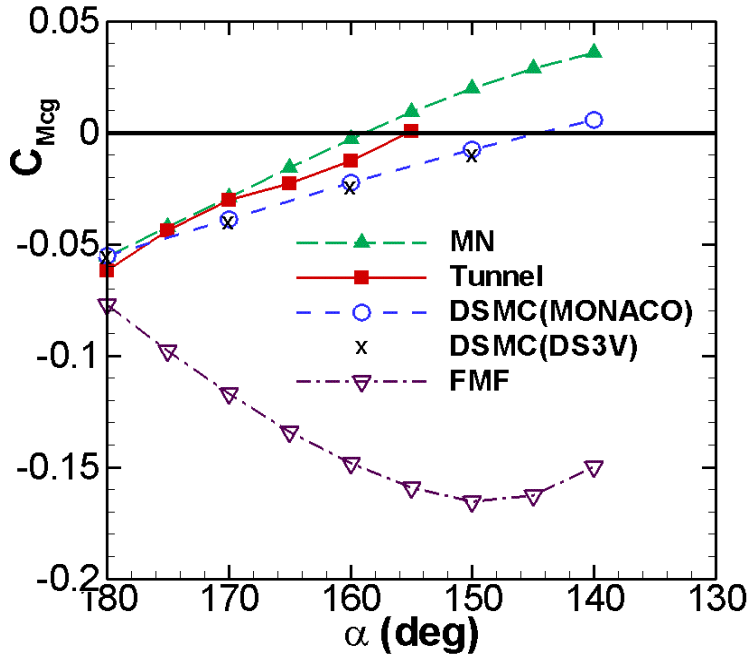

Figure 4c: Pitching moment for a capsule at angle of attack [30].

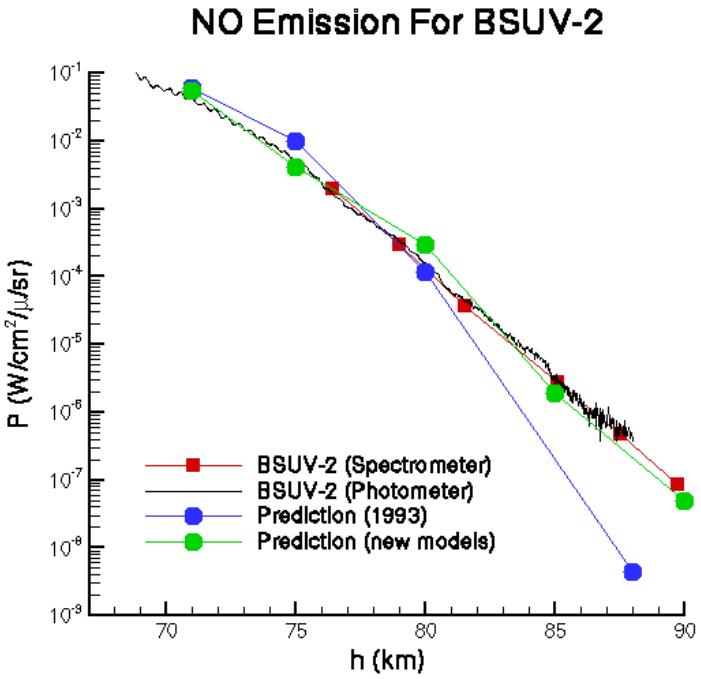

Figure 5a: NO emission as a function of altitude for the BSUV-2 hypersonic flight [38].

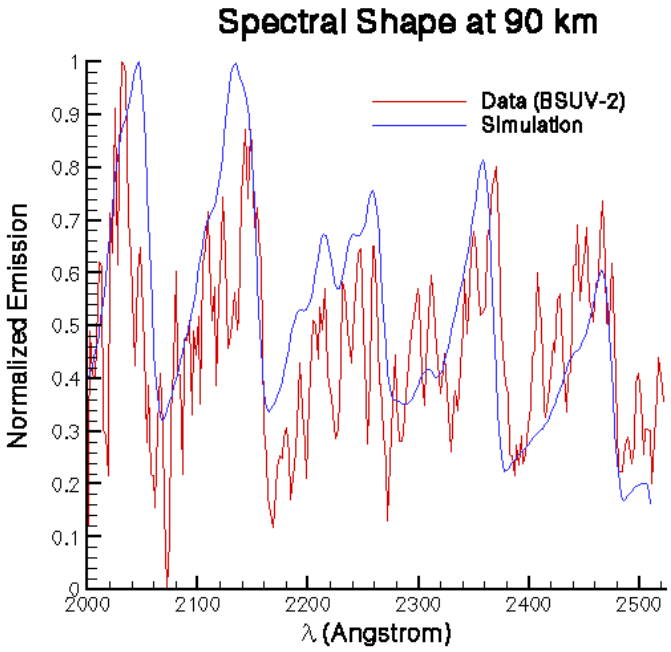

Figure 5b: Normalized NO spectra at an altitude of 90 km for the BSUV-2 flight [38].

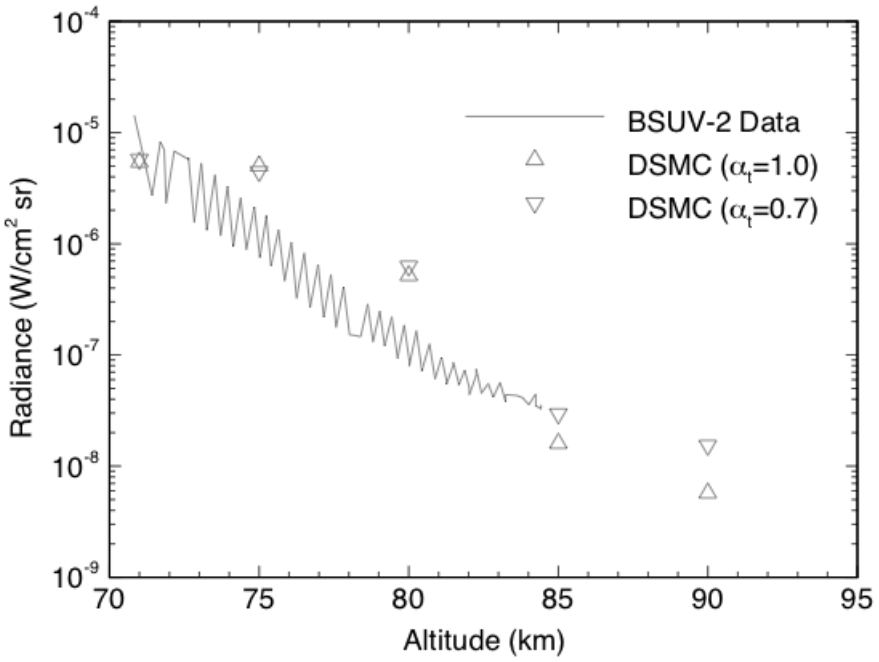

Figure 5c: O emission as a function of altitude for the BSUV-2 hypersonic flight [38].

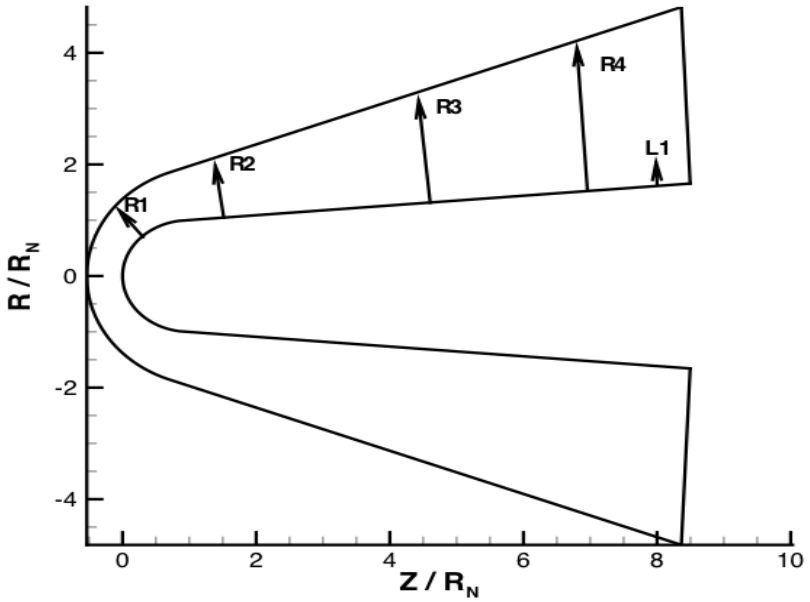

Figure 6a: RAM-C vehicle geometry and location of instrumentation.

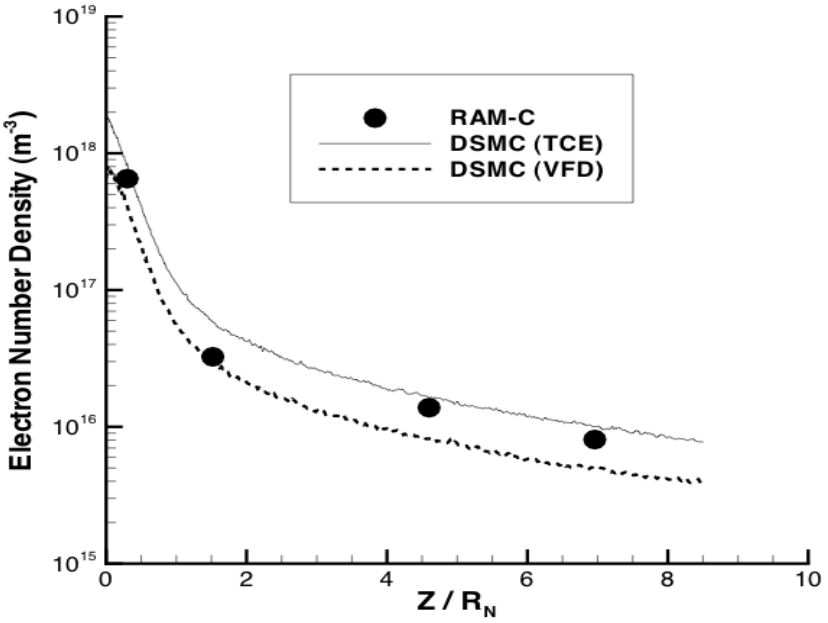

Figure 6b: Peak plasma density as a function of axial location along the RAM-C vehicle [41].

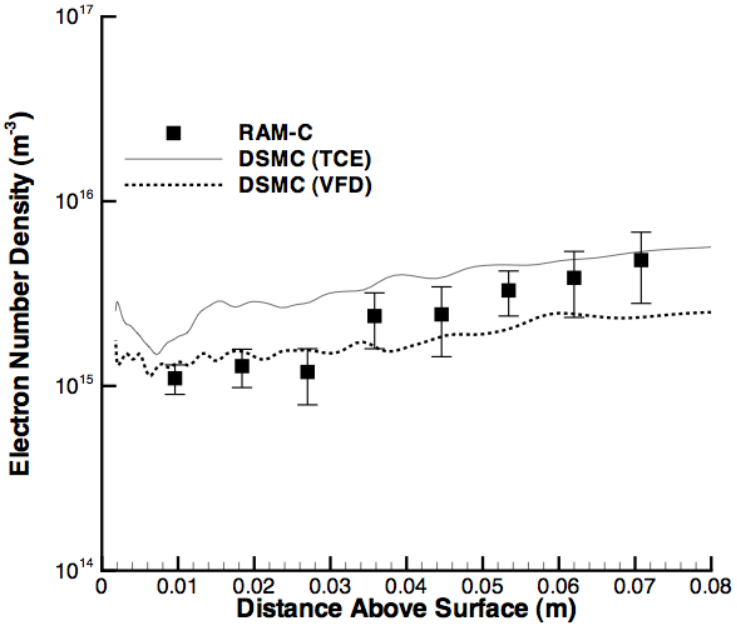

Figure 6c: Plasma density as a function of radial distance from the RAM-C surface [41].

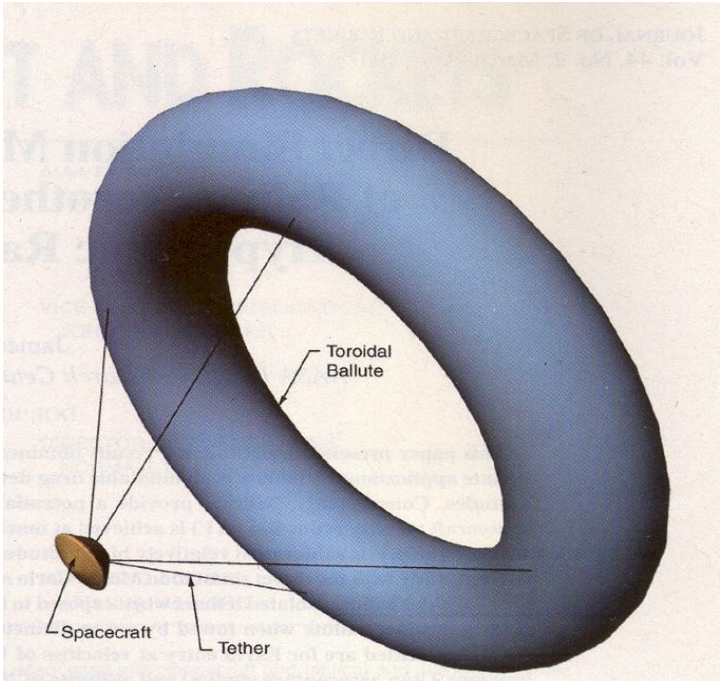

Figure 7a: Schematic diagram of capsule and ballute studied by Moss [45].

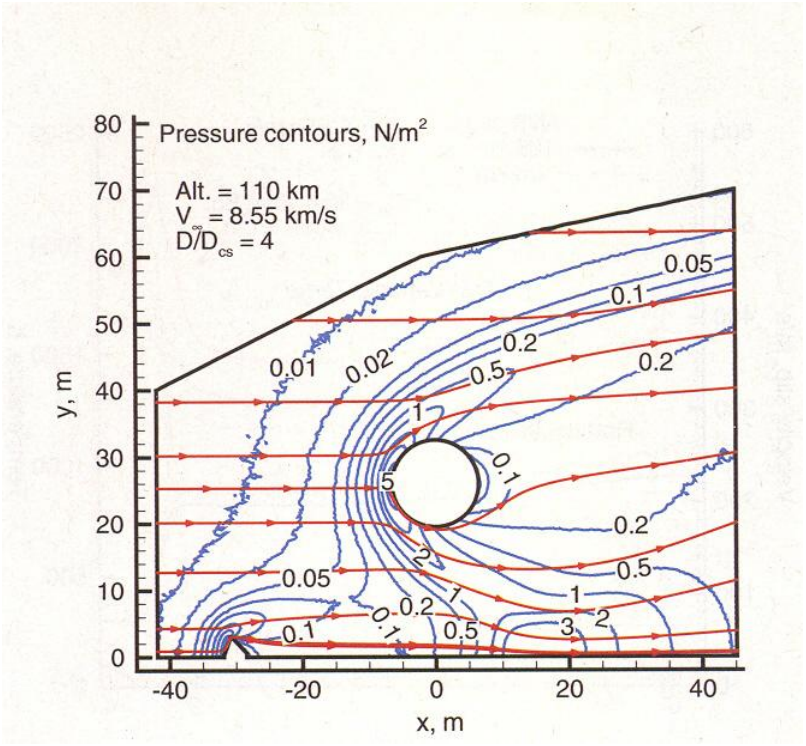

Figure 7b: Contours of pressure computed by Moss using DSMC about a capsule/ballute [45].

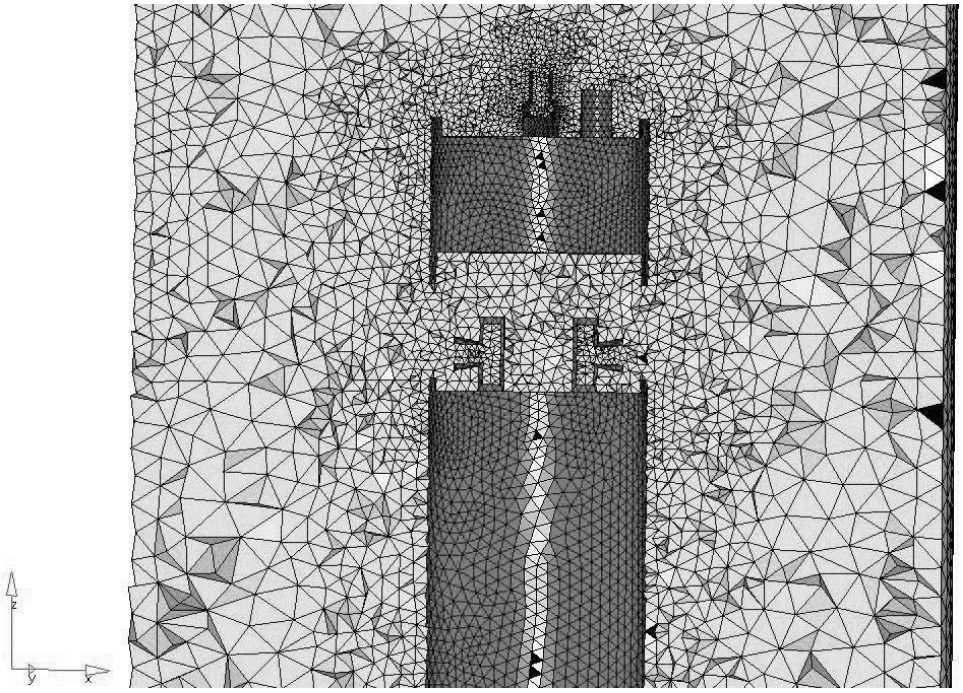

Figure 8a: Slice through the 3D tetrahedral mesh for TOMEX simulation [47].

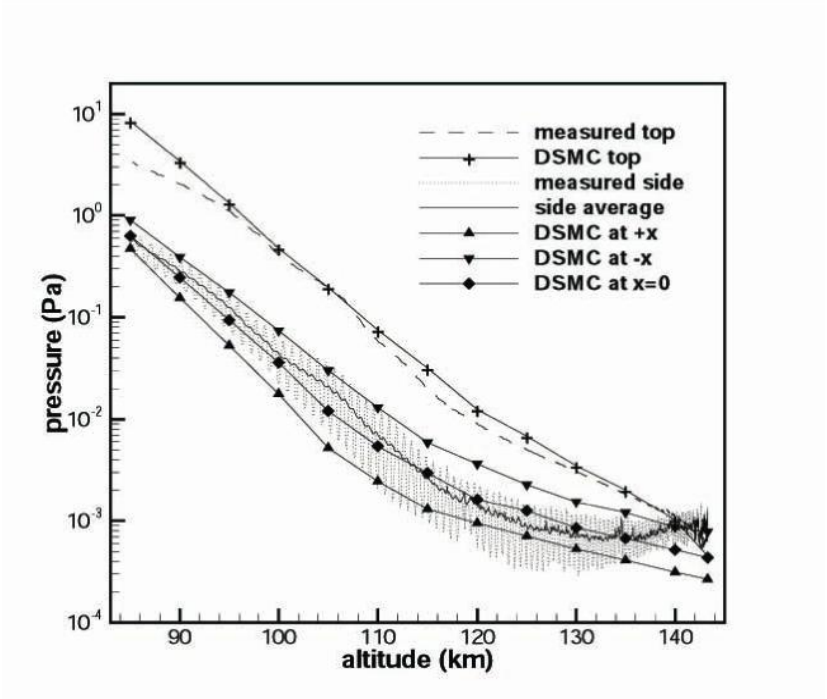

Figure 8b: Comparisons between TOMEX flight measurements and DSMC for pressure [47].

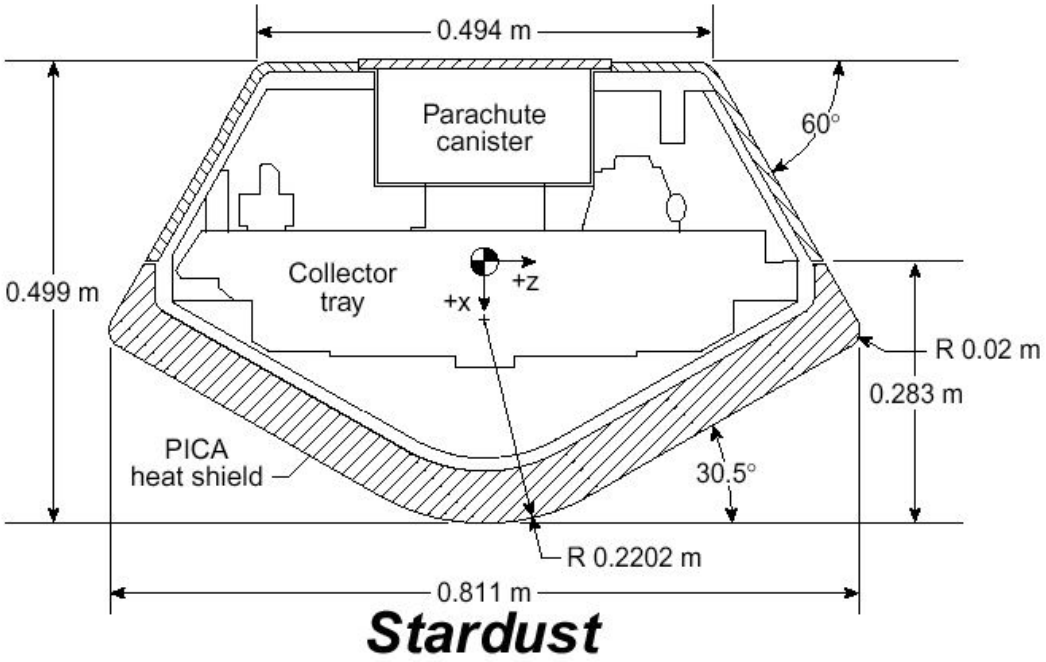

Figure 9a: Schematic diagram of the Stardust Sample Return Capsule (SRC).

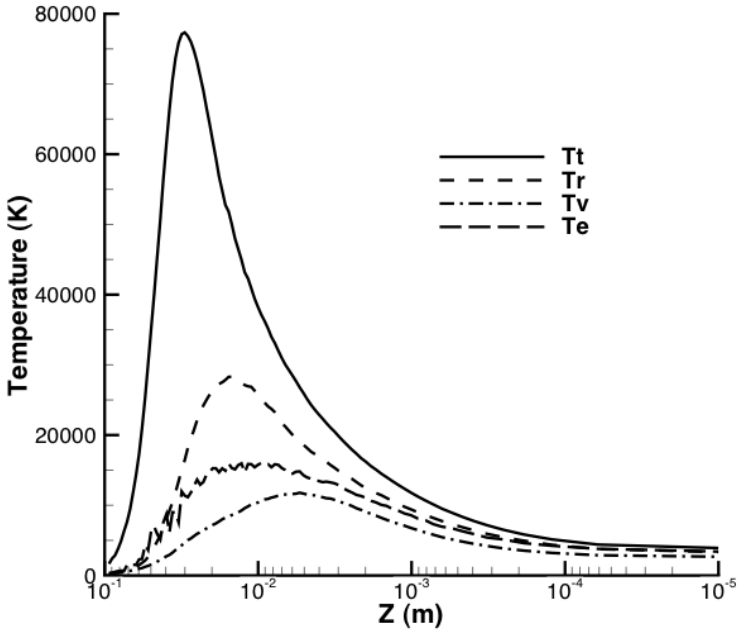

Figure 9b: Temperature profiles along the Stardust SRC stagnation streamline at 81 km [52].

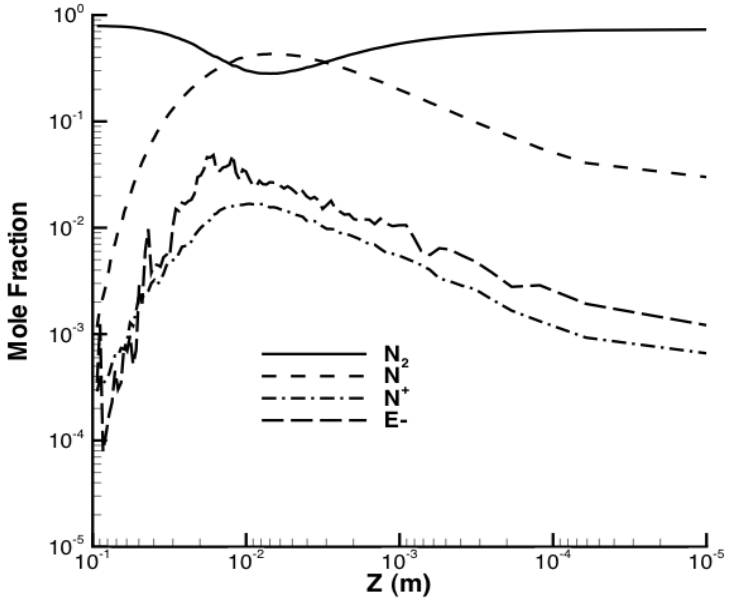

Figure 9c: Mole fraction profiles along the Stardust SRC stagnation streamline at 81 km [52].

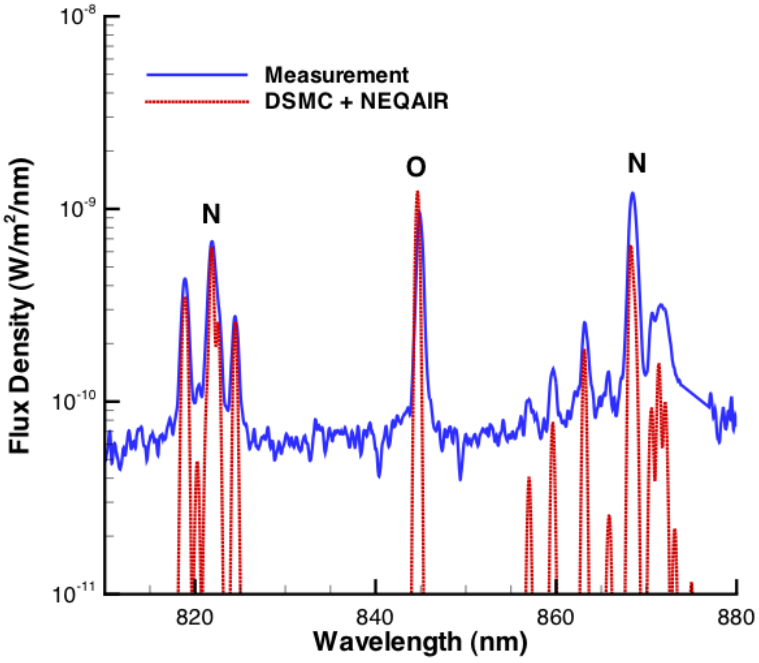

Figure 9d: Comparison of measured and computed spectra for Stardust at 81 km [52].

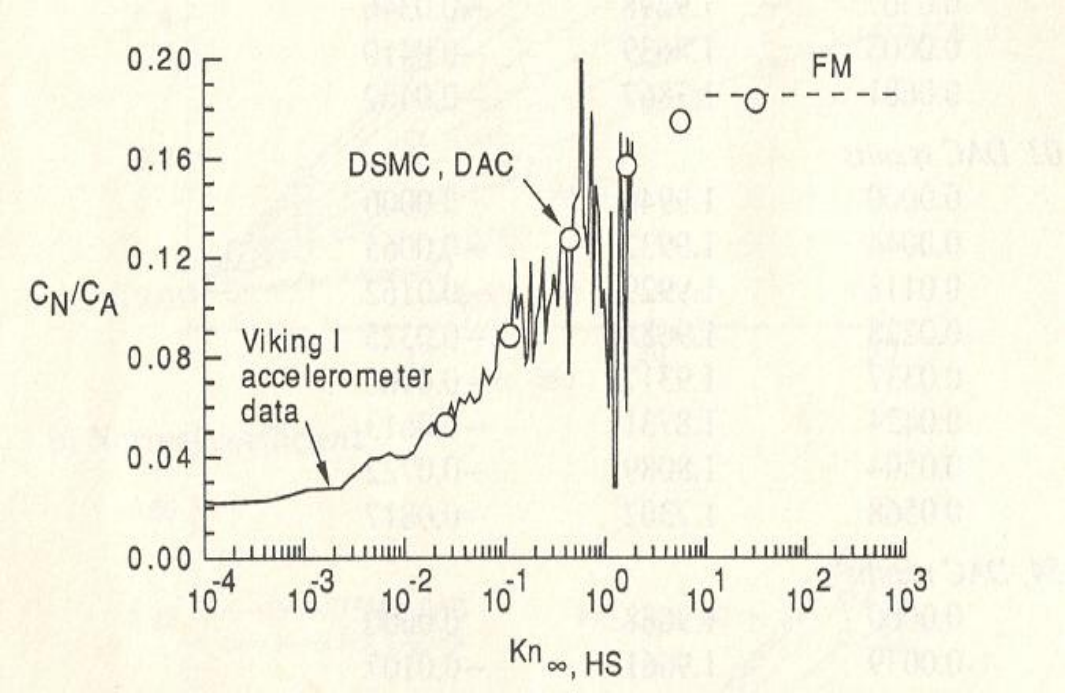

Figure 10: Ratio of normal-to-axial force coefficient for Viking I entry into Mars [53].

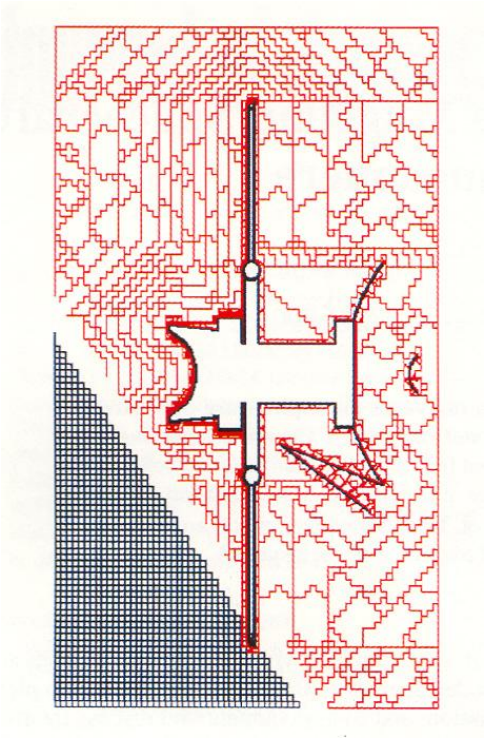

Figure 11a: Mesh employed by Rault to study Magellan orbiting Venus at 140 km altitude [57].

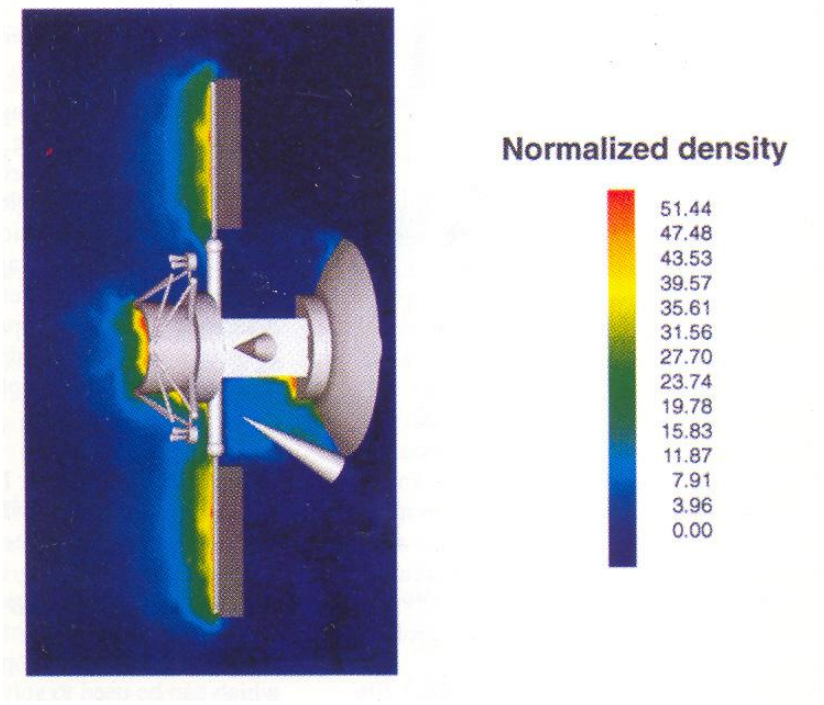

Figure 11b: Gas density around Magellan orbiting Venus at 140 km altitude [57].